Original Article

Institution of MECHANICAL ENGINEERS

Journal of RAIL AND RAPID TRANSIT

Proc IMechE Part F:
J Rail and Rapid Transit
2014, Vol. 228(6) 581–589

DOI: 10.1177/0954409714530911
pif.sagepub.com

SAGE

Investigation of the mechanics of rail seat deterioration and methods to improve the abrasion resistance of concrete sleeper rail seats

Ryan G Kernes, Amogh A Shurpali, J Riley Edwards, Marcus S Dersch, David A Lange and Christopher P L Barkan

Abstract

A sustained increase in gross rail loads and cumulative freight tonnages on heavy haul railways, as well as increased interest in high- and higher-speed passenger rail development, is placing an increasing demand on railway infrastructure and its components. Rail seat deterioration (RSD) refers to the degradation of the material at the contact interface between the sleeper's rail seat and the pad that protects the bearing area of the sleeper.

RSD continues to be identified as one of the primary factors limiting concrete sleeper service life, particularly in heavy haul operations. This paper includes results from two laboratory experiments that used test setups and protocols and were designed to isolate the abrasion mechanism. The first experiment was used to acquire quantitative and qualitative data related to the frictional properties of rail pad materials sliding on a concrete surface under various normal loads. The second experiment quantified the abrasion resistance of rail seat materials. Results confirmed that abrasion is a feasible RSD mechanism and that the frictional characteristics at the contact interface between the rail pad and concrete rail seat appear to have an impact on the transfer of forces and relative movement, and thus the abrasion mechanism. Also, the abrasion resistance of the rail seat's surface can be improved by grinding off the top cement paste layer to expose a hard aggregate surface and also by applying an epoxy coating to the surface. Increasing the service life of railway track components will facilitate capacity building on heavy haul, mixed-traffic and passenger railways around the world by reducing maintenance costs and decreasing the demand for maintenance windows.

Keywords

Concrete sleepers, track components, rail seat deterioration, abrasion, rail pad, concrete crosstie, coefficient of friction

Date received: 15 August 2013; accepted: 5 March 2014

Introduction

To meet the increasingly stringent design and performance requirements due to increasing axle loads and cumulative gross tonnages from heavy haul freight operations, along with increased high-speed inter-city passenger rail development, improvements in concrete crosstie designs are needed. These improved designs are especially critical on joint heavy haul freight and high-speed passenger rail infrastructure, where loading demands are highest, track geometric requirements are most stringent, and track occupancy time is at a premium. Improvements in concrete crosstie and fastening system designs also help address the need to reduce track maintenance windows, thereby gaining rail capacity.

Before these advancements are realized, several design and performance challenges must be overcome, including rail seat deterioration (RSD) and fastening system wear and fatigue.

RSD refers to the degradation of the concrete material at the contact interface between the crosstie rail seat and the rail pad.[1] RSD has been identified as one of the primary factors limiting concrete crosstie service life in North America, particularly in heavy haul freight infrastructure.[2,3] RSD can lead to problems such as loss of cant, gauge-widening, fastening system wear, and other track geometry deficiencies that create the potential for unstable rail conditions

Rail Transportation and Engineering Center, University of Illinois at Urbana-Champaign, USA

Corresponding author:
Ryan G Kernes, Rail Transportation and Engineering Center, University of Illinois at Urbana-Champaign, 3214 Newmark Civil Engineering Laboratory, 205 North Mathews Avenue, Urbana, IL 61801, USA
Email: rkernes2@illinois.edu

and/or derailments.[4] RSD is difficult to detect and impossible to repair without lifting the rail and removing the rail pad through a labor-intensive and costly repair process that results in track outages, traffic disruptions and increased operating costs. One of the primary maintenance challenges facing the rail industry is the lack of compatibility between life cycles of infrastructure components. If the life cycle of the materials that compose the rail seat and fastening system is not sufficient to match the life cycle of the rail, interim repairs of the rail seat may be necessary.

Background

The University of Illinois at Urbana-Champaign (UIUC) has identified five possible mechanisms that have the potential to contribute to RSD. These are abrasion, crushing, freeze-thaw cracking, hydraulic-pressure cracking and hydro-abrasive erosion. Of these mechanisms, hydraulic pressure cracking and hydro-abrasion have been investigated at UIUC and found to be feasible mechanisms resulting in RSD.[3,5,6] The work described in this paper seeks to build on previous research by focusing on the abrasion mechanism of RSD.

Abrasion is defined as the wear of materials as two or more surfaces move relative to one another.[6] Abrasion is a progressive failure mechanism and occurs when (i) cyclic motion of the rail base induces shear forces, (ii) shear forces overcome static friction, (iii) the pad slips relative to concrete, (iv) strain is imparted on the concrete matrix, and (v) the harder surface cuts or ploughs into the softer surface. The abrasive mechanism in RSD is further complicated and potentially accelerated due to the occurrence of three-body wear that results from the formation of an abrasive slurry, made up of fines and water, in addition to the two interacting surfaces (i.e. rail seat and rail pad).[7] A lack of understanding of the complex interactions affecting the severity of abrasion has resulted in an iterative design process for concrete crossties and fastening systems.

In order to improve our understanding of the interactions that lead to abrasion, two tests were designed and executed to understand and mitigate the abrasion mechanism in concrete sleeper rail seats. First, a large-scale abrasion test (LSAT) was developed to verify the feasibility of the abrasion mechanism and allow us to understand of the mechanics of abrasion by characterizing the frictional forces that resist movement at the contact interface between the concrete rail seat and the bottom of the rail pad.[8] Next, a small-scale test for abrasion resistance (SSTAR) was designed to understand the effect of various surface treatments on the abrasion resistance of the concrete rail seat. Although these results should be verified in full-scale tests, this small-scale test enabled us to compare methods of mitigating abrasion without the production of full-scale prototypes.

Laboratory experiment on the mechanics of abrasion

LSAT setup

The LSAT is made up of a test frame and two servo-hydraulic actuators. A servo-hydraulic actuator under displacement control provides the force needed to accelerate the pad perpendicular to the normal load and return the pad to its original position.

Simultaneously, an additional servo-hydraulic actuator under force control provides a static normal force on the pad, so that representative contact pressures can be maintained.

Both actuators are attached to a steel loading head that houses the abrasion pad in a recessed cavity. Mock concrete rail seat specimens that are 152 mm × 152 mm × 76 mm deep (6" × 6" × 3") are fixed to the floor via a steel base plate and adjustable angle supports. The pad materials are 76 mm × 102 mm × 19 mm thick (3" × 4" × 0.75") blocks of generic nylon 6/6 and polyurethane, approximately a quarter of the area of a typical rail pad. Water can be added through a channel within the loading head and can be deposited at the four edges of the pad through grooves in the top of the loading head cavity. Ottawa sand can be applied manually to the contact interface with a small measuring cup. A photograph of the test setup is shown in Figure 1.

Initially, a deterioration experiment was performed to verify that measurable abrasion could be caused with the test setup and to understand the input parameters that were the most critical to the severity of abrasion. Significant abrasion of the concrete specimens was achieved under a variety of normal loads, displacements, load rates and applications of sand and water.

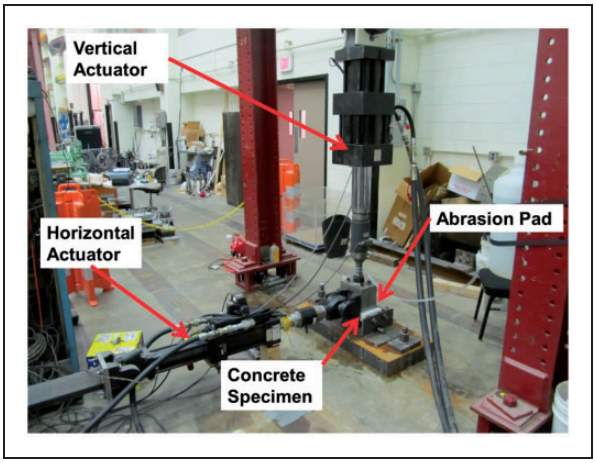

Figure 1. LSAT setup.

Efforts to correlate input parameters, such as the magnitude of displacement and normal force, with the severity of abrasion (wear depth) proved exceedingly difficult. In order to understand the mechanics of abrasion, additional variables were isolated and the testing protocol was simplified. Based on observations made during the deterioration tests, the frictional relationships that exist between rail pad materials and mock concrete rail seats appeared to change throughout the tests and vary based on a number of factors. Friction at the rail seat and rail pad interface appears to have an effect on the movement of the rail pad relative to the rail seat, the load transfer of wheel loads as they move from the top of rail through the fastening system components into the rail seat, and the abrasive wear behavior of both the rail pad and rail seat materials. Contrary to the deterioration experiment, where many thousands of loading cycles were necessary to understand the severity of progressive abrasion, observations related to the frictional characteristics can be made after any number of loading cycles. As a result, the testing procedure was designed to simulate a single train pass. It was hypothesized that the coefficient of friction (COF) would be reduced as the magnitude of the normal load on the pad was increased and the number of loading cycles performed during a single simulated train pass increased.

Experimental design

Normal load tests were performed to characterize the frictional forces of both nylon 6/6 and polyurethane pad materials. To evaluate the effect of increasing the normal load on the frictional coefficient between the pad and concrete surface, normal loads of 13 kN (3000 lbf), 22 kN (5000 lbf) and 44 kN (10,000 lbf) were applied to both pad types. Each pad and concrete specimen pair was tested four times at each load magnitude. Two sets of four tests were performed for both nylon 6/6 and polyurethane pads, resulting in a total of 16 tests of each pad type with no water or sand being added to the contact interface.

Testing protocol

A train was simulated by applying 400 loading cycles to the pad and concrete specimen, representing 100 four-axle rail cars. For each individual pad and concrete specimen, 400 lateral load cycles were applied at a frequency of 3 cycles/s (3 Hz) using the horizontally mounted actuator under displacement control. The magnitude of the displacement of the pad was fixed at 3.2 mm (1/8") and was achieved with a sinusoidal wave cycling with a 1.6 mm (1/16") amplitude. The vertical actuator under force control applied a specified normal load to the pad that essentially remained static throughout the test. The number of loading cycles and magnitude of displacement were fixed to reduce the number of variables relative to the deterioration experiment.

Throughout each test, a data acquisition system was used to record information from both actuators. The vertical force, P, and vertical displacement were recorded from the vertical actuator's load cell and linear variable differential transformer (LVDT), respectively. Similarly, the acquisition of data from the load cell in the horizontal actuator allowed us to constantly monitor the force, F, required to move the loading head to a specified position. The lateral displacement data were collected from the LVDT in the horizontal actuator.

The fundamental relationship for COF was used to calculate the COF (μ) each test

$$\mu = \frac{|F|}{P}$$

In order to monitor the thermal effects on the frictional behavior of the pad materials, the temperature of the pad surface was measured with an infrared thermometer before each test, and again as soon after the 400th cycle as it could be safely recorded.

The infrared thermometer had an internal laser to identify the target area.

The entire pad surface was scanned to find the maximum temperature. After the initial temperature, T_i, was measured, the normal load was applied to the pad using the vertical actuator. The position of the lateral actuator was verified so that the midpoint location of each test was consistent. Next, the data acquisition system was initiated and the function generator that controls the horizontal actuator was turned on. The horizontal actuator started at position 0, moved forward 1.6 mm, returned to position 0, and moved in the opposite direction for 1.6 mm for a total lateral displacement of 3.2 mm. After approximately 134 s, or 400 cycles, the test was stopped. Approximately 7 s passed between the last loading cycle and the time of the temperature measurement during which the cyclic motion of the lateral actuator was stopped and the loading head lifted to facilitate the temperature measurement. Once the loading head was retracted and the hydraulic system was turned off, the surface of the pad was scanned continuously in the same manner as prior to the test and the maximum detected temperature, T_f was recorded. Before the next test was started, the pad was allowed to cool to within 1 °C of its original starting temperature.

Results and discussion

The ratio of lateral load to vertical load was plotted at loading cycle 5, 100, 200, 300 and 400. Information from the first few loading cycles was difficult to interpret because these portions of the tests were not as

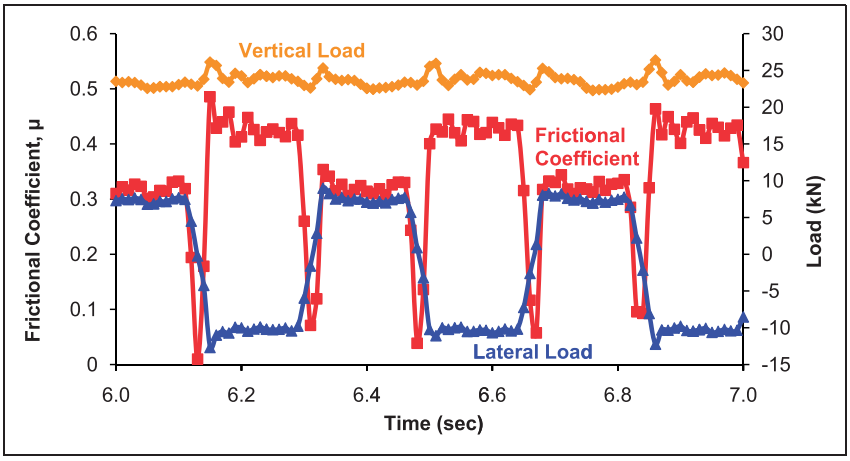

Figure 2. Sample values of the frictional coefficient, vertical load and lateral load obtained during three loading cycles.

repeatable as the remainder of the tests due to limitations of the testing equipment. The fixed connections on the equipment when combined with imperfect test specimens resulted in minor misalignments of the pad relative to the concrete. Typically, the minor misalignments were compensated and the test setup reached equilibrium after the first three loading cycles. Therefore, this analysis begins at loading cycle 5, which is the point where the results become highly repeatable. Nonetheless, when the pad slid relative to the concrete surface, the plot of lateral and vertical load relative to time showed repeatable behavior for the majority of the test duration. Upon plotting the calculated COF, a few general trends in the shape of the graph were observed. Figure 2 shows an example plot for three loading cycles that occurred during a friction test.

During the lateral movement phase of each cycle, the COF decreases slightly as the pad slides, where kinetic friction is resisting pad movement. As the movement of the loading head slows, so as to reverse direction, the magnitude of the lateral force drops to zero and there is a corresponding drop in the kinetic COF. At the end of each lateral displacement cycle, static friction resists pad movement and the COF value is at its highest magnitude just as the pad begins sliding in the opposite direction. The COF drops to zero again as the pad changes direction. This pattern is consistent with fundamental tribological principles, where the kinetic COF is expected to be lower than the static COF. The peak value for the COF during the specified loading cycle, between the changes in direction, was selected as the COF value for that loading cycle.

The most noticeable trend observed during the normal load tests is that the COF values appear to decrease as the loading cycles increase (Figures 3 and 4). Figures 3 and 4 show the mean values for all friction tests by normal force, with error bars that represent two standard errors for nylon 6/6 (Figure 3) and polyurethane pads (Figure 4). For both pad materials tested, a noticeable decline in the COF value was consistently observed from the beginning of each test (loading cycle 5) to the end of each test (loading cycle 400), and polyurethane exhibited higher COF values than nylon 6/6. Plastic deformation of the pad materials and concrete surface occurred at each load magnitude tested. Based on changes in surface color and reflectivity, the concrete appeared to be polished during tests at 13, 22 and 44 kN.

The decline in COF as a function of time during a simulated train pass is most likely due to the buildup of thermal stresses at the contact interface. Increases in the temperature of the pad at the local contact points were observed in all of the friction tests. T_f values as high as 77 °C were recorded on the surface of nylon 6/6 and 136 °C on the surface of polyurethane pads. The temperature build-up appeared to be localized to the primary load-bearing contact points on the pad. First, the shear strength of the pad material is likely being reduced at the contact interface as the temperature increase. Alternatively, the increases in temperature at local contact points may have resulted in the local melting of the pad materials that remain in the interface as a transfer film.[9,10] This transfer film can act as a lubricant, resulting in the reduction of the COF values.

The differences in COF values between nylon 6/6 and polyurethane can best be explained by the inherent properties of the materials that are a result of their crystalline structure and chemical characteristics. For this study, the most relevant property is shear modulus, which is a measure of the response of a material when a shear force is imposed. The published shear modulus of nylon 6/6 (1000 MPa) is approximately 20 times higher than the shear modulus of polyurethane (50 MPa) at 30 °C.[11] The shear moduli (both elastic and plastic) decrease as the temperature increases within the range of temperatures measured during the friction tests (24 to 172 °C). Although the polyurethane pads have a lower shear modulus, the COF values that were measured in this experiment were

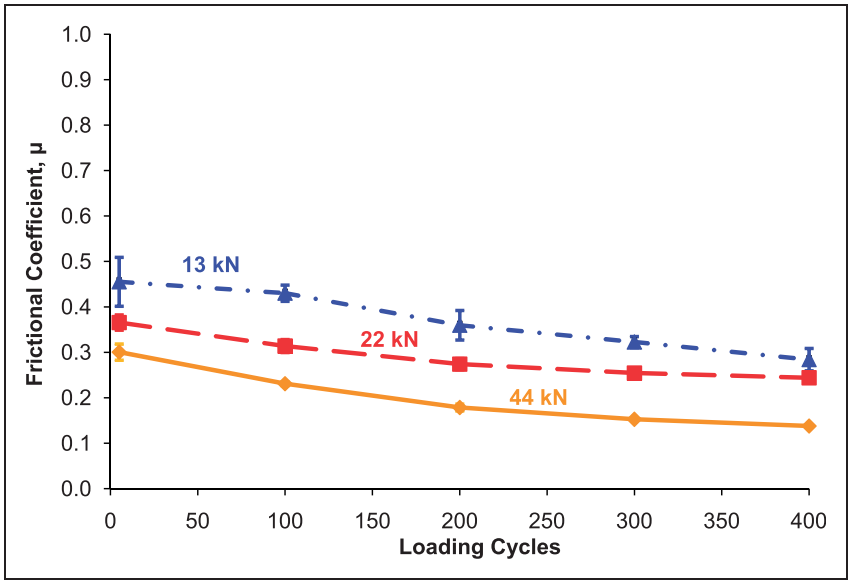

Figure 3. Mean COF values of nylon 6/6 pads under 13-, 22- and 44-kN normal loads.

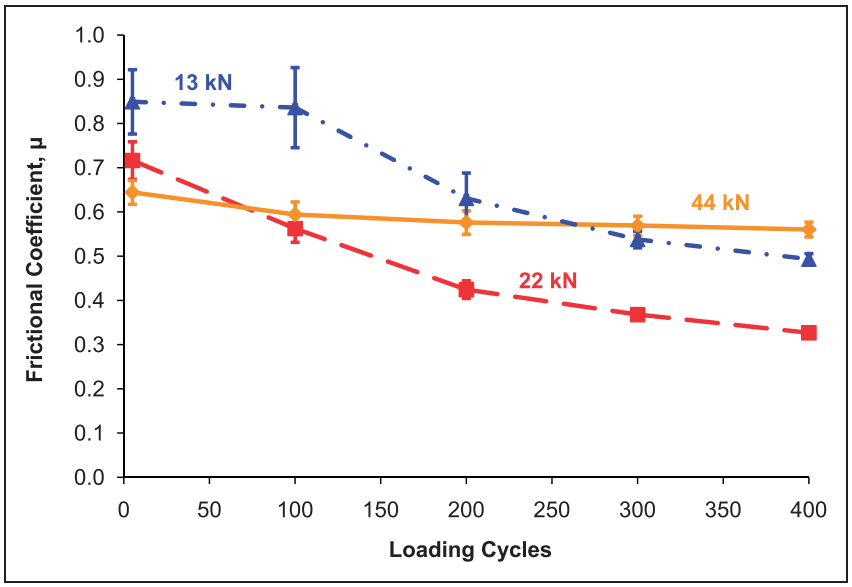

Figure 4. Mean COF values of polyurethane pads under 13-, 22- and 44-kN normal loads.

higher than those of nylon 6/6 pads. Therefore, secondary effects, such as the differences in the mechanics of the motion (e.g. internal shear, sliding), were likely governing the shear response.

As the magnitude of the normal force on the pads increased, the COF values generally appeared to decrease. The rate of the decrease in COF values was dependent on the pad material. The mean COF values in the 22-kN tests are lower than the 13-kN tests and higher than the 44-kN tests for nylon 6/6 pads. By contrast, the COF data for the polyurethane pads do not show a strong correlation between normal force and COF for tests with loads of 13 kN and 44 kN. The COF values at loading cycles 5 and 100 were lower at 44-kN loads than at 13-kN loads, but the COF values were higher at 44-kN loads than 13 kN and 22 kN by the end of the tests (Figure 4). However, the COF values for tests with a 22-kN normal force were consistently lower than the COF values for polyurethane pads loaded to 13 kN.

The nylon 6/6 pads displayed similar sliding behavior at 13 and 44 kN based on visual observations, but the frictional response of the pads under 44-kN normal loads yielded lower COF values. The COF recorded at 44 kN were consistently lower than those under a 13-kN load, including those recorded from a few trials on the same specimen that were tested in order to ensure that specimen-to-specimen variability was not affecting the perceived relationship between normal load and COF.

Table 1. Mean surface temperatures of pads as a function of the normal load.

Normal force (kN)	Nylon 6/6		Polyurethane	
	T_i (°C)	T_f (°C)	T_i (°C)	T_f (°C)
13	24	155	24	130
22	24	151	24	121
44	24	172	24	93

During the tests with a normal load of 44 kN, observations of the polyurethane pad under loading revealed that minimal sliding of the pad relative to the concrete was occurring. Instead, the pad appeared to absorb nearly all of the shear strain internally, that is within its own thickness, such that gross slip of the pad relative to the concrete was barely visible. As a result, the increase in temperature of these tests was significantly lower than in tests with 13-kN normal loads. The average temperature of 13-kN tests was 130 °C compared with 93 °C for 44-kN tests, which is a 28% decrease as a result of a 233% increase in normal load (Table 1). Additionally, less plastic deformation was visible on the pad surface after the 44-kN tests, in which minimal gross sliding was observed during the tests. Due to the combination of less slip, lower temperatures and less deterioration, the COF values under a 44-kN normal force remained relatively constant. These values are more representative of the internal shear properties of the pad than of the sliding frictional coefficient.

As the normal force on the pad material increased, the COF values decreased for pads that slid relative to the concrete. For plastic materials, the theoretical value of the COF is directly related to the true contact area and the shear strength, and is inversely proportional to the normal load.[12] Thus, the experimental relationship between load and COF measured in this study is in agreement with the theoretical tribology literature for polymer materials such as those tested. Since the actual contact area is extremely difficult to measure or estimate, the fundamental relationship of the ratio of lateral force to normal force was selected as the best method to calculate the COF in this study. Other experimental studies that utilized this method of calculating COF have reported a similar relationship between COF and normal force.[12-14]

The higher contact stresses that the pads experienced under increasing normal forces likely caused increased deformation at local contact points, thus changing the geometry of the contact and altering the shear behavior of the material. When the pressure exceeds a critical value that is based on the strength of a material, the friction and wear behavior of the polymer materials is affected.[15] The decreasing COF values with increasing normal load for both nylon 6/6 and polyurethane pad materials sliding on concrete demonstrate principles from tribology that are typically investigated for mechanical applications such as ball bearings.

Beyond the noticeable sliding of the pads, one of the most interesting observations in this experiment occurred on the softer pad material (polyurethane) under a 44-kN normal load. Nearly all of the deflection of the horizontal actuator (under displacement control) was taken internally, within the thickness of the pad, such that the pad did not appear to slide relative to the concrete. As a result, the calculated experimental COF values do not actually describe the frictional relationship. Instead, the internal shear properties of the polyurethane, lateral shear behavior versus normal force, are being described. Thus, the shear properties generally appeared to be constant throughout each of the 16 tests. This distinctly contrasts with the variable frictional relationship that was observed in experiments that resulted in sliding pads. The fact that a large shear force can be input into the top of the pad material, absorbed within the 6 mm thickness of polyurethane, with minimal slip on the concrete, may have large implications on the shear contact behavior of rail pads. Based on these results, frictional characteristics at the contact interface between the rail pad and concrete rail seat likely vary and affect the deformation of the rail pad. Therefore, the frictional properties at this interface should be accounted for in the shear design of the rail pad.

Laboratory test results for improved rail seat materials

The LSAT presents a novel approach to the RSD problem, and includes representative component materials (e.g. nylon and concrete) and conditions that are representative of the field (e.g. rail seat pressures, abrasive slurry). However, there are limitations to large-scale testing, which require more time and resources to operate, and can present challenges when investigating component-level behavior within the system. These challenges limit the breadth, depth and effectiveness of a parametric study to identify ways of mitigating RSD. The aforementioned limitations and lessons learned from previous test development led UIUC researchers to the development of a simplified test known as the SSTAR.

The SSTAR was designed with the following characteristics: 1. the ability to isolate the abrasion mechanism, 2. ability to quantify the abrasion resistance of different concrete specimens, 3. comparatively simple and economic to operate, 4. allows for shortened testing durations that facilitate the collection of large volumes of data.

Two surface treatments, epoxy coating and exposed aggregate, were tested to quantify their abrasion resistance and assess the feasibility of each approach to mitigate the effects of abrasion.

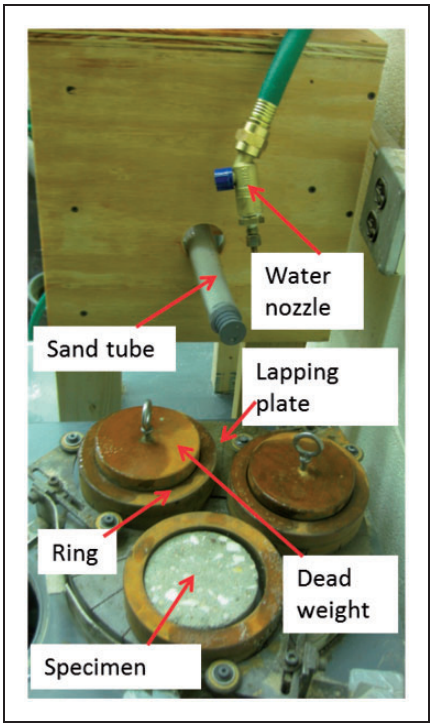

Figure 5. SSTAR test setup.

In North America, epoxy coatings are frequently used as a reactive RSD repair material and/or preventative RSD mitigation measure. Preliminary qualitative results from revenue testing have been promising according to Class I railroads. An exposed aggregate surface can be achieved by grinding the top layer of cement paste at the rail seat to expose a relatively uniform plane composed of coarse and fine aggregate materials. Since aggregates are generally harder and more durable than cement paste, an exposed aggregate surface was tested in this study in order to determine if a significant improvement in abrasion resistance is feasible.

SSTAR test setup

The SSTAR was constructed by modifying a lapping machine that is typically used to sharpen tools or create flat, smooth surfaces on machined metal parts, and for rock polishing in geotechnical engineering (Figure 5). The lapping machine is comprised of a revolving steel plate with concrete specimens loaded in three counter-rotational rings that rest on the plate and are held in place relative to the rotating disk. The three rings are held in place on the lapping plate by small rubber wheels attached to the main frame. This allows the circular specimens to revolve around their center while still maintaining the same position relative to the revolving lapping plate. A dead weight of 2 kg (4.5 pounds) is placed on top of each specimen. To represent the influence of water and fines that are often seen in the field, an abrasive slurry, consisting of water and Ottawa sand, is applied to the lapping plate throughout the test to abrade the concrete surface that mates against the lapping plate.

SSTAR test protocol

First, samples were cast using a concrete mix-design that is representative of a mix used for the manufacture of concrete crossties in North America. Specimens cast with this control mix design (cured in 100% humidity) will hereafter be referred-to as "control specimens". Any change in abrasion resistance is measured relative to the control specimens.

In order to have satisfactory confidence in our test results, nine specimens (or replicates) were tested for each rail seat surface treatment. The concrete specimens were marked to identify the wearing surface (i.e. the as-cast surface). Initial thickness values at four marked locations were obtained using a pair of vernier calipers. Three specimens were then placed on the lapping machine rings, the deadweight was applied, and the test was started. At the same time, the abrasive slurry was introduced into the specimen–lapping plate interface.

After testing, the wear depth data (i.e. difference between initial and final thickness values) was plotted with respect to testing duration to represent the progression of abrasion with time.

Further details regarding the rationale behind the development of the test, test apparatus construction, specimen production, test protocol and preliminary results from previous testing can be found in a previous publication.[10]

Results and discussion

Wear depth is used as a metric to quantify abrasion and is the inverse of abrasion resistance. Figure 6 shows wear rate curves for specimens wherein each data point represents the average value of data obtained from nine specimens. Error bars representing two standard errors (positive and negative) in wear depth are shown on all data points. As curves shift downward on the graph, the surface material shows higher abrasion resistance.

Data from the SSTAR shows that epoxy coating improves the abrasion resistance of concrete by approximately 10% relative to control specimens (Figure 6). It was also observed that the epoxy coating quickly disintegrated and added to the abrasive slurry once it developed cracks. The abrasive wear rate matched that of control specimens after the epoxy coating was completely lost. This phenomenon can likely be attributed to the hardness and smooth finish of the brittle epoxy coating layer. However, the use of an epoxy coating could still be cost-effective if it delays the onset of RSD, and increases the life cycle of concrete crossties. The improvement in abrasion resistance due to exposing the aggregate was

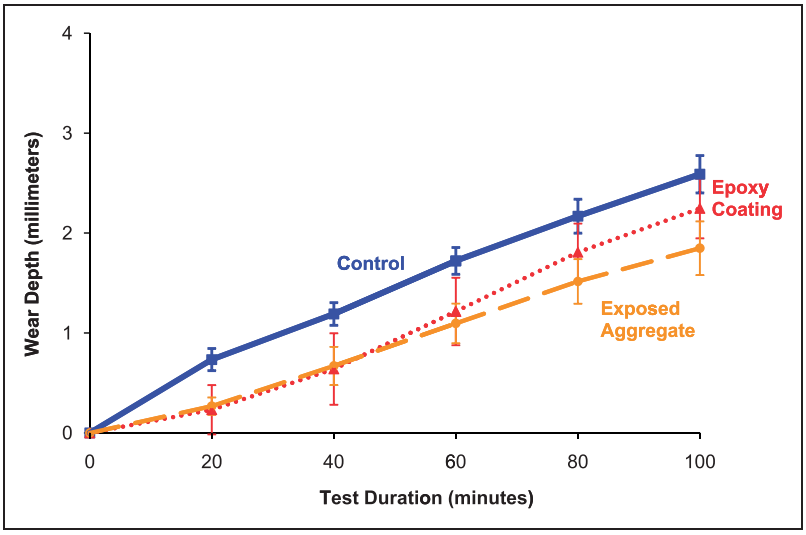

Figure 6. The average value of the wear depths obtained for each surface treatment.

13.5% greater than that of the epoxy-coated specimens. As mentioned earlier, this is likely due to the harder, durable aggregate being exposed instead of concrete paste.

Conclusions

Experiments performed on the LSAT confirmed that abrasion is a feasible RSD mechanism. Based on the results of these experiments, the frictional characteristics at the contact interface between a rail pad and concrete rail seat appear to have an impact on the transfer of forces and relative movement, and thus the abrasion mechanism. The properties of rail pads, such as the shear modulus, flexural modulus, hardness and geometry appear to affect frictional behavior. In addition, temperature changes that can occur due to repeating loading cycles and the magnitude of the normal force appear to impact the shear contact behavior at the rail seat interface. Increases in temperature can affect the material properties of the pad material. Finally, increasing pressures due to higher normal forces may increase the propensity of the pad to slip relative to the concrete due to a reduction of the COF, thus exacerbating the demands on the rail seat.

Through experimental testing using the SSTAR, researchers at UIUC have successfully compared two approaches to improving the abrasion resistance of the rail seat. Data from SSTAR illustrates that the abrasion resistance of the rail seat's surface can be improved by grinding off the top cement paste layer to expose a hard aggregate surface and applying an epoxy coating to the surface. Although these results should be verified in full-scale tests, this small-scale experiment enabled us to prioritize methods of mitigating abrasion before proceeding with the production of full-scale prototypes. The knowledge gained from this research will be used to help formulate specific recommendations to mitigate the adverse effects of RSD in future, both from the rail pad as well as the concrete materials standpoint.

Funding

The authors would like to express sincere gratitude to the Association of American Railroads (AAR) Technology Scanning Committee and the NEXTRANS Region V Transportation Center for sponsoring this research. J. Riley Edwards was supported in part by grants to the UIUC RailTEC from CN, CSX, Hanson Professional Services, Norfolk Southern, and the George Krambles Transportation Scholarship Fund.

Acknowledgements

The authors would like to thank Amsted RPS, Amsted Rail, VAE Nortrak and KSA for providing us with critical resources for the laboratory experimental work. Special thanks go to Dave Bowman and Jose Mediavilla (Amsted RPS) and Steve Mattson (VAE Nortrak) for providing direction, advice, and encouragement. Many thanks to the members of AREMA Committee 30, including John Bosshart, Greg Grissom, Eric Gehringer, Scott Tripple, Bob Coats and Pelle Duong. This work would not have been possible without contributions from Tim Prunkard, Darold Marrow, Don Marrow, Emily Van Dam, Xiang Liu, Brandon Van Dyk, Sam Sogin, Greg Frech, Chris Rapp, Calvin Nutt, and Ryan Feeney (UIUC).

References

1. Kernes RG, Edwards JR, Dersch MS, et al. Investigation of the Impact of abrasion as a concrete crosstie rail seat deterioration (RSD) mechanism. In: *The American Railway Engineering and Maintenance of Way Association (AREMA) conference,* Minneapolis, MN, 18–21 September 2011. Landover, MD: AREMA.

2. Edwards JR, Dersch MS and Kernes RG. UIUC FRA concrete tie and fastener BAA (2014). Unpublished report for the Federal Railroad Administration. University of Illinois at Urbana-Champaign, USA, 2012. Washington DC: United States Department of Transportation.
3. Zeman JC. *Hydraulic mechanisms of concrete-tie rail seat deterioration*. Master's Thesis, University of Illinois at Urbana-Champaign, USA, 2010.
4. Zeman JC, Edwards JR, Dersch MS, et al. Failure mode and effect analysis of concrete ties in North America. In: *Proceedings of the ninth international heavy haul conference*, Shanghai, China, 22–25 June 2009, pp.270–277. Beijing: China Railway Publishing House.
5. Bakke KJ. Abrasion resistance. In: Lamond JF and Pielert JH (eds) *Significance of Tests and Properties of Concrete and Concrete-Making Materials*. West Conshohocken, PA, 2006, pp.184–193. Bridgeport: ASTM International.
6. Choros J, Marquis B and Coltman M. Prevention of derailments due to concrete tie rail seat deterioration. In: *The ASME/IEEE joint rail conference and the ASME Internal Combustion Engine Division conference*, Pueblo, CO, 13–16 March 2007, pp.173–181. Beijing, China: China Railway Publishing House.
7. Dwyer-Joyce RS, Sayles RS and Ioannides E. An investigation into the mechanisms of closed three-body abrasive wear. *Wear* 1993; 175: 133–142.
8. Kernes RG, Edwards JR, Dersch MS, et al. Investigation of the impact of abrasion as a concrete crosstie rail seat deterioration (RSD) mechanism. In: *American Railway Engineering and Maintenance of Way Association (AREMA) conference proceedings*, Minneapolis, USA, 18–21 September 2011, pp.18–21. Landover: AREMA.
9. Badhadur S. The development of transfer layers and their role in polymer tribology. *Wear* 2000; 245: 92–99.
10. Srinath G and Gnanamoorthy R. Effect of short fibre reinforcement on the friction and wear behaviour of nylon 66. *Appl Compos Mater* 2005; 12: 369–383.
11. BASF Polyurethanes GmbH. CAMPUS datasheet Elastollan 1195 A, http://www.campusplastics.com/campus/en/datasheet/Elastollan%C2%AE+1195+A/BASF+Polyurethanes+GmbH/59/b5a54956 (2012, accessed 31 January 2012).
12. Yamaguchi Y. *Tribology of plastic materials*. Amsterdam, The Netherlands: Elsevier, 1990, pp.1–13.
13. Srinivasan V, Asaithambi B, Ganesan G, et al. Mechanism of glass fiber reinforced epoxy composites under dry sliding using fuzzy clustering technique. *J Reinf Plast Compos* 2009; 28: 1349–1358.
14. Wantanabe M and Yamaguchi H. The friction and wear properties of nylon. *Wear* 1986; 110: 379–388.
15. Anderson JC. The wear and friction of commercial polymers. In: Friedrich K (ed.) *Friction and wear of polymer composites*. Amsterdam, The Netherlands: Elsevier, 1986, pp.329–362.
16. Shurpali AA, Edwards JR, Lange DA, et al. Laboratory investigation of the abrasive wear mechanism of concrete crosstie rail seat deterioration (RSD). In: *The ASME/ASCE/IEEE 2012 Joint rail conference*, Philadelphia, PA, 17–19 April 2012.